New Journal of Physics
The open-access journal for physics

Structure and diffusion of small Ag and Au clusters on the regular MgO (100) surface

G Barcaro and A Fortunelli[1]
Molecular Modeling Laboratory, IPCF-CNR, Via G. Moruzzi 1, Pisa, I56124, Italy
E-mail: fortunelli@ipcf.cnr.it

New Journal of Physics **9** (2007) 22
Received 6 October 2006
Published 8 February 2007
Online at http://www.njp.org/
doi:10.1088/1367-2630/9/2/022

Abstract. The lowest energy structures and the diffusion energy barriers of small $M_N (N = 1–4)$ Ag and Au clusters absorbed on the regular MgO (100) surface are investigated via density-functional (DF) calculations, using two different xc-functionals (PBE and LDA). In agreement with previous work, it is found that the lowest-energy structures of Ag and Au clusters in this size-range exhibit a strong 'metal-on-top' effect, by which the clusters are absorbed atop oxygen ions in a linear (dimer) or planar (trimer and tetramer) configuration perpendicular to the surface. The corresponding diffusion mechanisms range from monomer hopping, to dimer leapfrog (Ag_2) or hopping (Au_2), trimer walking, tetramer walking (Ag_4) or rocking and rolling (Au_4), exhibiting interesting differences between Ag and Au. An analysis of the corresponding energy barriers shows that trimers can diffuse at least as fast as monomers, while tetramers and (especially in the case of gold) dimers present somewhat higher barriers, but are anyway expected to be mobile on the surface at the temperatures of molecular beam epitaxy (MBE) experiments. The calculated PBE diffusion energy barriers compare reasonably well with the values extracted from the analysis of recent MBE experimental data, with the LDA predicting slightly higher barriers in the case of gold.

[1] Author to whom any correspondence should be addressed.

PII: S1367-2630(07)34447-9

Contents

1. Introduction

Metal clusters absorbed on oxide surfaces [1, 2] have been the subject of growing attention in recent years due to their interest in many scientific and technological fields, ranging from catalysis and chemical sensing [3]–[10] to optoelectronic and electrical devices [11]–[14], etc. A key issue in this respect is represented by the control of the size and distribution of the clusters, i.e., of the growth process, in its various components: absorption, diffusion, nucleation and sintering. As the field grows mature, the initial emphasis on the energetics of static processes, such as absorption and nucleation [15]–[19], is gradually shifting and extending to more complex dynamical processes, such as diffusion [20, 21] and sintering [22]. In particular, as emphasized in [23], the role of small cluster diffusion in affecting the growth kinetics is not fully understood, and deserves further investigation. In close analogy with the field of the dynamical processes of metal atoms and clusters on metal surfaces [24, 25], the first studies have appeared [26]–[29] in which the mechanism and kinetics of diffusion of metal adatoms and metal clusters on oxide surfaces were investigated in detail. The main result of these studies [27, 28], as applied to the prototypical Pd/MgO (100) system—probably the most well-known metal-on-oxide model catalyst [30]—was that mobility of small clusters is important to understand the growth of Pd islands on MgO (100), and that only by explicitly considering these processes can theoretical predictions and experimental observations be fully reconciled. In this respect, it is therefore interesting to know whether the Pd/MgO (100) system represents an exceptional case, or whether the overall picture can be extended to other systems. In particular, it is of interest to know how fast dimers and larger clusters can move, and by which mechanisms. In the present study, we address these issues by reporting the results of density-functional (DF) calculations aimed at determining the lowest-energy structures and diffusion energy barriers of small $M_N (N = 1–4)$ silver and gold clusters on the regular MgO (100) surface. Gold and silver clusters absorbed on MgO (100) are of interest for their peculiar chemical [3], [5]–[7], [31, 32] and optical [11]–[14], [33] properties, and have thus been intensively studied in recent years [17], [32]–[44]. Moreover, silver and gold are noble metals, with an electronic configuration of the single atoms ($d^{10}s^1$)

different from that of Pd ($d^{10}s^0$), and thus represent interesting examples for testing whether small metal cluster mobility is confirmed in these cases.

The paper is organized as follows. In section 2, the computational details are presented. In section 3, the results of the DF calculations are reported, distinguished in terms of nuclearity to help the comparison between silver and gold and with the experimental data [21]. Finally, conclusions are summarized in section 4.

2. Computational details

The DF calculations for the determination of the lowest-energy structures are performed using the plane-wave self-consistent field (PWscf) computational code [45] employing ultrasoft pseudopotentials. The Perdew–Burke–Ernzerhof (PBE) exchange-correlation functional [46], which is a gradient-corrected (GGA) functional, is used; in some calculations also the local density approximation (LDA) functional [47] is used. The kinetic energy cutoff for the selection of the plane-wave basis set is fixed to 40 Ryd (1 Ryd ≈13.6 eV) for all the calculations. A (3,3,1) *k*-point sampling of the Brillouin zone is chosen, and a Gaussian smearing procedure (with a smearing parameter of 0.002 Ryd) is applied. The geometry optimizations are stopped when the maximum force on the atoms is less than 10^{-4} au. The regular MgO (100) surface is modelled by a three-layer slab (as is customary [38]), each layer containing 9 Mg and 9 O atoms fixed at the equilibrium lattice positions characterizing the MgO rock-salt structure (with lattice parameter equal to the experimental value of 4.208 Å). The distance between metal atoms in replicated cells is at least 4–6 Å.

The determination of the diffusion barriers is performed by applying the climbing image nudged elastic band (CI-NEB) [48, 49] module of the PWscf package. This method searches for the minimum-energy path between two local minima of the potential energy surface (PES) by creating a fixed number of intermediate configurations (images) which are linked to each other by elastic springs. After a few iterations, the band-tangent component of the force felt by the image highest in energy (the climbing image) is inverted and this image is set free to evolve towards the *true* saddle point along the pathway. In our calculations, five images have been chosen; the first and the last are two local minima singled out from the lowest-energy structures of the metal clusters located by the previous search.

It should be noted that we only evaluate the diffusion energy barriers and not the Arrhenius prefactors. A full evaluation of the kinetic constants for diffusion would in principle imply also an estimate of these entropic factors, for example—applying the transition state theory [50]—by calculating the ratio of the vibrational frequencies of the normal modes at the minima and at the saddle points [28, 29]. However, we chose not to perform the corresponding calculations because: (i) the entropic factors evaluated through the transition state theory using atom–atom potentials [51] were substantially constant for the diffusion processes investigated in the present study; (ii) in the case of Pd, the entropic factors did not qualitatively modify the results, bringing about differences smaller than the intrinsic accuracy of the DF approach (see later the differences between the LDA and PBE approaches). Along the same lines is the choice of not relaxing the MgO coordinates. Firstly of all, unconstrained DF theory using GGA (such as PBE) xc-functionals (at variance with hybrid xc-functionals [52]) makes the MgO system rather soft, whereas by employing a GGA xc-functional and fixing the oxide lattice parameter at the experimental value one partially recovers the hard character of the oxide [53]. Secondly,

we do not expect the relaxation of the oxide coordinates to qualitatively modify our results, as suggested by the comparison with the case of palladium clusters on MgO (100), both as far as the lowest-energy structures and the diffusion energy barriers are concerned [27, 28] (note that the Pd/surface interaction is even stronger than that of coinage metals). Indeed, as will be shown below, the DF/PBE energy barrier for the diffusion of a single Au atom is 0.22 eV from our calculations, in which the MgO surface is kept fixed, and 0.24 eV from the calculations of [38], obtained using an equivalent computational approach, but in which the oxide coordinates are fully relaxed.

3. Results and discussion

Our aim is to locate the lowest-energy local minima of small Ag and Au clusters on the MgO (100) surface and to find the lowest-energy diffusion pathways connecting them.

For each local minimum, it is convenient to define four quantities: (i) the adhesion energy (E_{adh}), calculated by subtracting the energy of the oxide surface and of the metal cluster, both frozen in their interacting configuration, from the value of the total energy of the system; (ii) the binding energy of the metal cluster (E_{met}), calculated by subtracting the energy of the isolated metal atoms from the total energy of the metal cluster in its interacting configuration; (iii) the metal cluster distortion energy (E_{dist}), which corresponds to the difference between the energy of the metal cluster in the configuration interacting with the surface, and the energy of the cluster in its lowest-energy gas-phase configuration; and (iv) the total binding energy (E_{bnd}), which is the sum of the binding energy of the metal cluster and of the adhesion energy ($E_{\mathrm{bnd}} = E_{\mathrm{adh}} + E_{\mathrm{met}}$).

For each diffusion pathway we report the value of the energy barrier, calculated using the CI-NEB method [49]. The results of subsections 3.1–3.4 have been obtained using the PBE xc-functional, those in subsection 3.5 using the LDA xc-functional.

To better compare the behaviour of silver and gold, the results are distinguished in terms of nuclearity (N) for the clusters Ag_N and Au_N, with $N = 1$–4.

3.1. Single atoms

As shown in [16, 17, 34, 37, 38, 40, 42, 44], for both Ag and Au single atoms the highest value of the adhesion energy to the regular surface corresponds to the absorption on top of an oxygen ion of the terrace. The preferential absorption on this site is a common feature of all neutral transition metal atoms, and, in the case of Au, it has been experimentally demonstrated [54]. In the case of the coinage metals (Cu, Ag and Au), the interaction is rather weak, less than 1 eV at the PBE level, because of the remarkable repulsion between the diffuse unpaired s electron of the metal and the charge density of the oxide surface, as discussed in [16, 17, 34, 40, 42]. Within the group, Au is characterized by the strongest adhesion (about 0.9 eV at the DF/PBE level), because the relativistic contraction of the s orbital brings it to overlap with the d orbitals of the metal [55]: the resulting s–d mixing means that the electronic density of the metal can be polarized away by the electric field of the surface in the outward direction, and, as a consequence, the metal orbitals are partially depleted and can accept charge density from the oxide surface [16, 17, 34, 38, 40, 42]. The total charge transfer between the Au atom and the MgO surface is however small [54]. On the contrary, Ag is characterized by the weakest interaction (about 0.4 eV) because of the poor hybridization between the s and d orbitals (for Ag, the low lying d orbitals are well separated

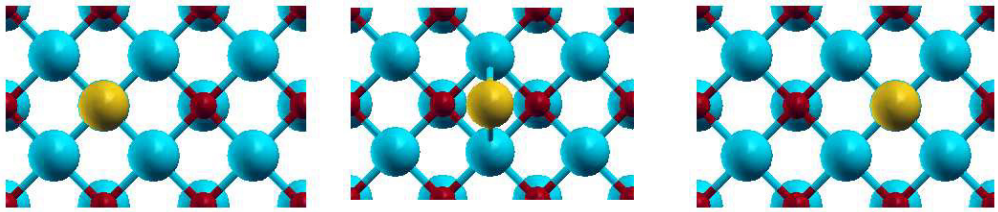

Figure 1. Schematic representation of the monomer hopping diffusion mechanism.

from the s orbital). The diffuse character of the valence s electron is further responsible for the stronger repulsion between the metal electronic cloud and the oxide charge density [34, 39, 42]. The diffusion of the single atom then takes place through a hopping mechanism (see figure 1) [38, 43]: the metal atom moves from one oxygen site to one of its four first neighbours passing above a hollow site, which represents the saddle point of the movement, in close analogy with the Pd case [27, 28, 56]. The diffusion energy barrier is thus easily determined by evaluating the difference in adhesion energy between the oxygen site and the hollow site. From our calculations, this difference amounts to 0.22 eV in the case of Au and 0.10 eV in the case of Ag, respectively (see tables 1 and 2), which compares very well with previous estimates [38, 43]. Thus the weaker adhesion of silver determines also a smaller value of the diffusion barrier. The value for Au is in reasonable agreement with the experimental data: it has been observed, in fact [62], that Au starts being mobile around 100–130 K on the regular MgO (100) surface, implying an energy barrier in the range 0.2–0.3 eV.

3.2. Dimers

At variance with the case of Pd_2 [57], the dimers of silver and gold are absorbed in an upright position perpendicular to the surface atop an oxygen site of the terrace, as already shown in [35, 37, 38, 42, 44]. This configuration is stabilized by an electrostatic contribution deriving from the increased polarization of the metal electronic density of the dimer in the field of the oxide. In general, it has been noted [36]–[39] that the presence of metal atoms above those directly interacting with the surface *increases* the adhesion energy (this effect is what we have called the 'metal-on-top' stabilization mechanism [37]).

The configurations that have been considered for the dimers and the corresponding diffusion pathways are displayed in figure 2. The energy analysis is reported in table 1.

In the case of gold, the metal-on-top effect in the ground-state configuration is so strong that the adhesion of the dimer is 1.41 eV, which corresponds to an *increase* of 0.5 eV with respect to the adhesion of the single atom, despite the fact that the atom interacting with the surface is involved in a strong metallic bond, which should *decrease* its availability to interact with the surface, in substantial agreement with previous analyses [35, 38]. The other two configurations that have been considered are: (b) an epitaxial one with two metal atoms absorbed atop two first neighbour oxygens on the surface, previously considered in [35]; (c) a configuration where the dimer is perpendicular to the surface but atop the hollow site. In configuration (b), which represents a local minimum, due to the stickiness of the metallic bond

Table 1. The values of the various energy quantities defined in the text are reported for the lowest-energy structures and saddle points for Ag_N and Au_N ($N = 1$–4) clusters, as calculated using the PBE xc-functional. The notation (a)–(e) refers to the configurations reported in figures 1–4.

Cluster	Configurations	E_{adh} (eV)	E_{met} (eV)	E_{dist} (eV)	E_{bnd} (eV)
Au_1	Oxygen	0.91	–	–	0.91
Au_1	Hollow	0.69	–	–	0.69
Ag_1	Oxygen	0.43	–	–	0.43
Ag_1	Hollow	0.33	–	–	0.33
	(a)	1.41	2.33	0.00	3.74
Au_2	(b)	0.56	2.31	0.02	2.87
	(c)	0.79	2.33	0.00	3.12
	(a)	0.66	1.73	0.00	2.39
Ag_2	(b)	0.44	1.73	0.00	2.17
	(c)	0.41	1.73	0.00	2.14
Au_3	(a)	1.52	3.58	0.01	5.10
	(b)	1.72	3.52	0.07	5.24
Ag_3	(a)	0.90	2.60	0.01	3.50
	(b)	0.91	2.58	0.03	3.49
	(a)	1.86	6.03	0.16	7.89
	(b)	2.18	5.86	0.32	8.04
Au_4	(c)	0.85	5.33	0.86	6.18
	(d)	1.44	6.16	0.03	7.60
	(e)	1.46	6.18	0.01	7.64
	(a)	1.00	4.55	0.03	5.55
	(b)	1.11	4.40	0.18	5.51
Ag_4	(c)	0.87	3.72	0.85	4.60
	(d)	0.92	4.58	0.00	5.50
	(e)	0.89	4.57	0.00	5.46

the equilibrium distance of the dimer (around 2.5 Å) is only slightly elongated with respect to the gas-phase, and the two metal atoms cannot match very well the two oxygens of the terrace (which are at a distance of about 2.97 Å). In this configuration the metal-on-top effect is completely absent and the adhesion energy (0.56 eV) is decreased by 0.85 eV with respect to the ground-state. In configuration (c), which represents a saddle point, the loss in adhesion energy (0.62 eV) is larger than the difference in adhesion between the oxygen site and the hollow site for the single atom (about 0.2 eV). The decrease in the adhesion is thus mainly due to a decrease of the metal-on-top effect when passing from the oxygen to the hollow site, probably because of the different form of the electric field above the two sites. The hopping mechanism with the dimer passing through the hollow site keeping the axis perpendicular

Table 2. The values of the energy barriers for the various diffusion mechanisms considered in the text are reported for Ag_N and Au_N ($N = 1$–4) clusters, as calculated using the PBE xc-functional.

Cluster	Mechanism	Barrier (eV)
Au_1	Monomer hopping	0.22
Au_2	Dimer hopping	0.62
Au_2	Dimer leapfrog	> 0.87
Au_3	Trimer walking	0.19
Au_4	Tetramer walking	0.60
Au_4	Tetramer rocking/rolling along [100]	0.44
Au_4	Tetramer rocking/rolling along [110]	0.42
Ag_1	Monomer hopping	0.10
Ag_2	Dimer hopping	0.25
Ag_2	Dimer leapfrog	0.22
Ag_3	Trimer walking	0.12
Ag_4	Tetramer walking	0.21
Ag_4	Tetramer rocking/rolling along [110]	0.58
Ag_4	Tetramer rocking/rolling along [100]	0.55

to the surface corresponds exactly to the energy difference between the ground-state and configuration (c), and amounts to 0.62 eV. Another possible diffusion mechanism is a 'leapfrog' movement with the dimer passing from the ground-state (a) to configuration (b) and again to the ground-state but atop an oxygen first neighbour of the starting one: the barrier has not been explicitly calculated using the CI-NEB approach, as it is necessarily higher than the energy difference between the ground-state and configuration (b), i.e., 0.87 eV. The leapfrog mechanism has previously been suggested as the lowest-energy diffusion mechanism for the Cu_2 dimer on a regular MgO (100) surface [26]; the dimer hopping mechanism, instead, has not been described before. We can thus conclude that the diffusion of the gold dimer is characterized by a barrier (0.62 eV) higher than the one characterizing the diffusion of the single atom (0.22 eV).

The case of silver is not qualitatively different as far as the static structures are concerned: the ground-state, configuration (a), is stabilized by the metal-on-top effect in the upright position perpendicular to the surface [42, 57]. The gain in adhesion with respect to the single atom is lower than in the case of gold, which implies that silver is characterized not only by a weaker direct interaction, but also by a weaker polarization contribution. This fact determines that configuration (b), the epitaxial one, and (c), the vertical one atop the hollow site, are characterized by a moderate loss of adhesion energy with respect to the ground-state: 0.22 and 0.25 eV, respectively (see the detailed analysis in table 1). The diffusion barrier for the vertical diffusion is equal to the difference between the ground-state and configuration (c), and amounts to 0.25 eV. The diffusion through the leapfrog mechanism, which in this case has been evaluated through the CI-NEB approach, is characterized by a barrier almost identical to the energy difference between the ground-state and configuration (b), i.e., 0.22 eV. As in the case of gold, the barrier for the diffusion of the dimer (0.22 eV) is thus higher than the one for the single atom (0.10 eV).

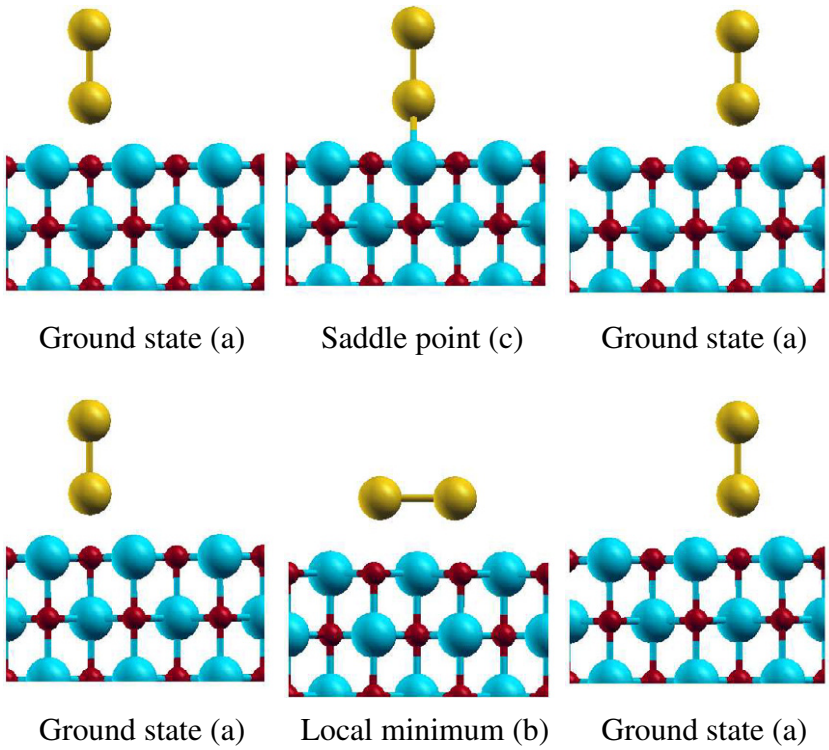

Figure 2. Schematic representation of the dimer hopping diffusion mechanism (first row) and of the dimer leapfrog diffusion mechanism (second row).

3.3. Trimers

In analogy with the Pd_3 case [58], the trimers of silver and gold are absorbed in an upright position with the cluster plane perpendicular to the surface and two metal atoms interacting with two oxygen ions of the terrace, as already shown in [35, 37]. The plane of the trimer can be oriented along the [110] direction—configuration (a), see figure 3—with the two basal metal atoms atop two first neighbour oxygens, or it can be oriented along the [100] direction—configuration (b)—with the two basal metal atoms pointing towards two oxygen atoms at a distance of 4.21 Å and with a magnesium atom underneath the centre of mass of the cluster. Configuration (a) has been considered in previous studies [35, 37], finding energy values in reasonable agreement with the present results, whereas, to our knowledge, configuration (b) has so far been neglected. The two configurations can be approximately interconverted through a rotation of 45° around an axis perpendicular to the surface and passing through one of the basal atoms of the cluster. In both the Ag and the Au case, the energy difference between the two configurations is very low: both structures are stabilized by the metal-on-top effect; moreover, the trimer, characterized by a doublet spin state, is a Jahn–Teller system with one electron occupying an anti-bonding orbital and is thus highly fluxional both in the gas-phase and when absorbed on the surface [37]. In the case of gold, configuration (b) is lower in energy than configuration (a) by 0.14 eV. In the case of silver, the two configurations have practically the same energy. An analysis of the energy contributions for the two configurations for both metals is reported in table 1.

Trimer diffusion can take place through successive transformations of configuration (a) into (b); this is obtained by a rotation of 45° around one of the two basal atoms, see figure 3. This

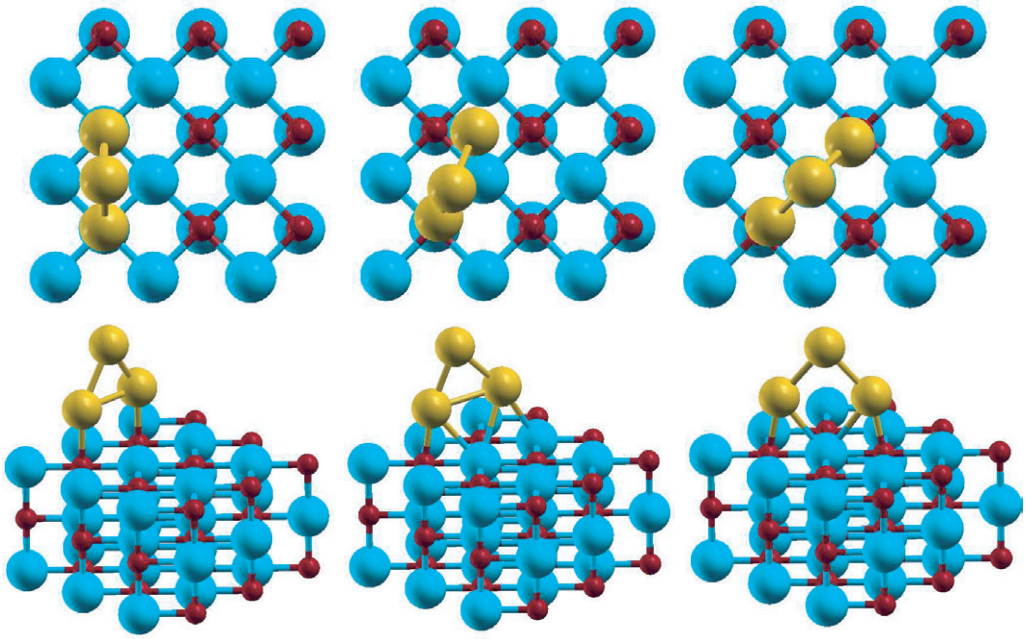

Figure 3. Schematic representation of the trimer walking diffusion mechanism.

kind of movement, already found in the case of the cluster Pd_3 [27, 28] on a (100) MgO surface, can be called *trimer walking*, and it takes place with the cluster keeping its plane perpendicular to the surface. The saddle point has been determined for the two metals by applying the CI-NEB method and corresponds to an intermediate angle of rotation between the two minima. The energy barrier amounts respectively to 0.19 eV in the case of Au_3 and 0.12 eV in the case of Ag_3, respectively. The two values are similar to the values found for the diffusion of the single atoms. In particular, in the case of gold, the barrier for the trimer is slightly lower than that of the monomer (0.19 eV versus 0.22 eV).

3.4. Tetramers

The lowest energy structures and saddle points of the gold and silver tetramers are displayed in figure 4, while the corresponding energies are reported in table 1.

The results for the tetramer are partly similar to the results found in the case of the trimer, but with interesting differences. We start the discussion by considering Au_4. In the two lowest-energy local minima, labelled (a) and (b) in figure 4, the cluster has the shape of a rhombus (the same shape characterizing the global minimum in the gas-phase) and interacts with the surface through two basal metal atoms. If the cluster plane is oriented along the [100] direction, we find the global minimum, configuration (b), whereas, if the plane is oriented along the [110] direction, we find a local minimum higher in energy by about 0.15 eV, configuration (a), which has been already considered in a previous study [36], which found energy values in reasonable agreement with the present results. These two configurations can be obtained from the configurations (a) and (b) of the trimer by absorbing a fourth atom in a metal-on-top position (not in direct contact with the surface). The ordering between the two configurations is the same as in the case

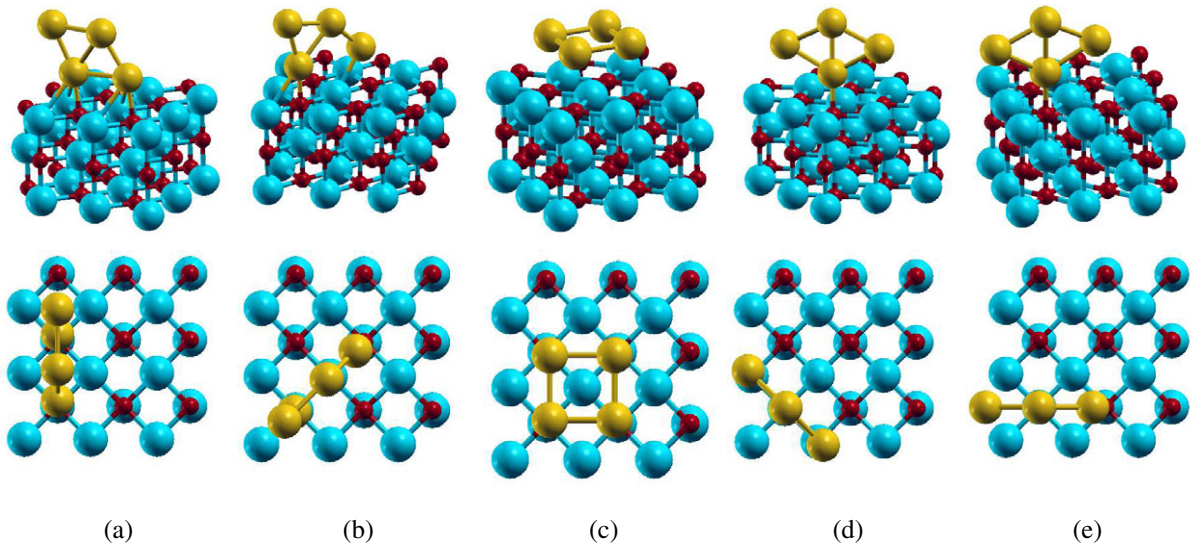

Figure 4. Schematic representation of the lowest-energy structures (a, b) and saddle points (d, e) of Ag and Au tetramers on a regular MgO (100) surface. Configuration (c) is a local minimum at higher energy.

of the trimer, and their energy difference is also very similar (0.15 eV versus 0.14 eV). The most significant difference with respect to the case of the trimer is that the tetramer undergoes a significant distortion, as can be noted in figure 4, in passing from the gas-phase to being absorbed on the surface, with distortion energies of 0.16 eV in configuration (a) and 0.32 eV in configuration (b), respectively. This is due to the fact that the tetramer is a closed shell with a reduced fluxional character with respect to the trimer. The loss of metallic energy is compensated in both configurations by the enhanced adhesion to the surface due to the metal-on-top effect. Another local minimum is configuration (c), where the tetramer has the shape of a square and is absorbed on four oxygen ions of the terrace. This configuration is strongly destabilized with respect to the previous ones, because of a significant loss in both metallic energy and adhesion energy. The low value of the adhesion energy of this structure is a further confirmation that the metal-on-top effect accounts for an important contribution to the adhesion: structure (c), with four atoms in direct contact with the surface, has an adhesion energy almost three times smaller than the adhesion of configuration (b), where the cluster is in direct contact with only two oxygen atoms. The last two configurations considered, (d) and (e), are saddle points: they have a C_{2v} symmetry, and interact with the surface with only one metal atom. They only differ between each other by the orientation of the cluster plane, which is along the [100] direction for configuration (d) and along the [110] direction for configuration (e). They are both characterized by lower values of distortion energies, but also lower values of the adhesion to the surface. Configuration (e) has already been considered in previous studies [36, 57].

The results for Ag_4 are qualitatively very similar. As can be noted from the values reported in table 1, all the configurations—except configuration (c)—are characterized by a value of the total binding energy of about 0.1 eV, because of a compensation between the metallic bond and the adhesion contributions. Also in this case, configurations (a) and (b) are the lowest-energy minima, but now, at variance with the case of Au, configuration (a) is the global minimum and configuration (c) is slightly higher in energy. Configurations (d) and (e), instead, are saddle

points. It is interesting to note that, for silver, the adhesion energy of configuration (c) is not much smaller than the adhesion of the other configurations and that the main loss is due to the destabilization of the metallic bond. This is again an indication that the metal-on-top effect is weaker in the case of silver with respect to gold and of the same order of magnitude as the direct interaction. The weak global adhesion to the surface is also suggested by the lower values of the distortion energies with respect to the gold tetramer: an appreciable loss of metallic bond is favourable only when it is compensated by a significant interaction with the surface.

The diffusion of the tetramer can take place through a variety of mechanisms, all of which are novel, as a rhombic configuration adhering through one of its edges is peculiar to silver and gold. One possibility is represented by a movement of 'tetramer walking' between configurations (a) and (b), a movement analogous to trimer walking. The difference with respect to the trimer is that the rotation of 45° can take place either around the vertex at higher coordination or around the vertex at lower coordination: the two movements have different barriers as it is energetically less costly to move the basal atom with lower coordination with respect to the basal atom with higher coordination, because the former loses less 'metal-on-top' or metal-bonding stabilization energy. In the case of gold, the values of the two energy barriers are 0.38 and 0.60 eV, respectively; in the case of silver 0.10 and 0.21 eV. Since a tetramer needs both movements for real diffusion (a single rotation does not allow the cluster to leave an area of four first-neighbour oxygen sites) the real value of the barrier is thus 0.60 eV for gold and 0.21 eV for silver. Therefore, despite the similarities between the walking mechanisms in the trimers and tetramers, the need to move an atom with higher coordination makes the diffusion energy barrier for the tetramer higher than that for the trimer. However, while in the case of silver the tetramer walking mechanism corresponds to the diffusion mechanism with the lowest barrier, in the case of gold we have found other processes characterized by lower activation energies. In figure 5, in fact, we can see how the configuration (b) can move along the [100] direction to another configuration (b) through a rocking mechanism, i.e., passing through the saddle point (1)—barrier of 0.39 eV—or through a rolling mechanism, i.e., passing through the saddle point given by configuration (d)—barrier of 0.44 eV. The rolling movement (to be distinguished from a qualitatively different movement of the Pd_4 tetrahedron [27, 28]) consists of revolving the cluster around the most coordinated atom in direct contact with the surface. The combination of these two movements determines a diffusion of the tetramer along the [100] direction; the barrier is given by the higher value between the the two values found: 0.44 eV. Still another possibility is that configuration (b) first rotates into configuration (a) through the first step of the walking mechanism, and that configuration (a) then diffuses through successive rocking/rolling movements along the [110] direction in a way completely analogous to the diffusion of configuration (b) along the [100] direction. Configuration (a) thus flips into another configuration (a) through the saddle point (2)—barrier of 0.27 eV—and rolls into another configuration (a) through the saddle point (e)—barrier of 0.25 eV.[2] The barrier for this mechanism is given by the sum of the energy difference between configuration (a) and (b)—0.15 eV—and the higher of the two rocking/rolling barriers—0.27 eV, for a total of 0.42 eV. The rocking/rolling processes in the two directions are thus energetically equivalent and both very favourable with respect to the walking mechanism. These rocking/rolling movements are not competitive in the case of silver because they pass through the saddle points (1) and

[2] We note that the energy difference between the (a) and (e) configurations obtained in [36] through a DF/BP86 method using a cluster approach is appreciably larger, probably due to the choice of the xc functional.

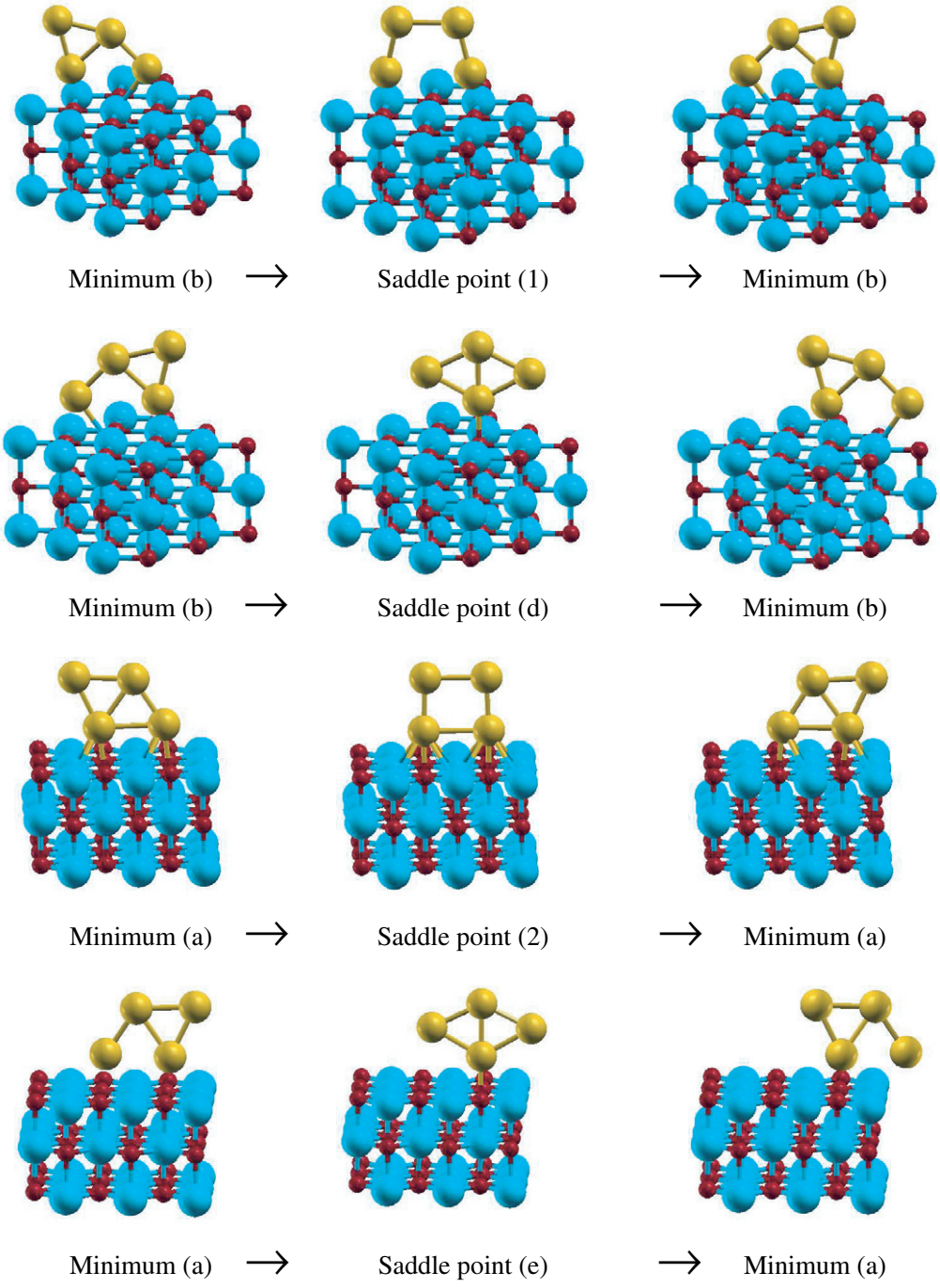

Figure 5. Schematic representation of the rocking/rolling diffusion mechanism along the [100] direction (first and second row) and along the [110] direction (third and fourth row).

(2) which present a remarkable distortion of the metal bonding, a distortion not compensated by an enhanced direct adhesion nor by the metal-on-top effect. Despite the similarities between Ag and Au, we can thus find subtle differences in the diffusion behaviour of the two metals.

Table 3. The values of the various energy quantities defined in the text are reported for the lowest-energy structures and saddle points for $Au_N (N = 1–4)$ clusters, as calculated using the LDA xc-functional; the notation (a)–(e) refers to the configurations reported in figures 1–4.

Cluster	Configurations	E_{adh} (eV)	E_{met} (eV)	E_{dist} (eV)	E_{bnd} (eV)
Au_1	Oxygen	1.54	–	–	1.54
Au_1	Hollow	1.26	–	–	1.26
	(a)	2.14	2.97	0.00	5.11
Au_2	(b)	1.44	2.93	0.04	4.37
	(c)	1.39	2.97	0.00	4.36
Au_3	(a)	2.71	4.87	0.04	7.58
	(b)	2.97	4.73	0.18	7.70
	(a)	3.11	8.13	0.21	11.24
	(b)	3.51	7.85	1.00	11.36
Au_4	(c)	2.23	7.34	1.47	9.57
	(d)	2.32	8.31	0.03	10.63
	(e)	2.36	8.34	0.00	10.70

The results of the energy barriers for the diffusion mechanisms described up to now are summarized in table 2. It can be noted that, for both metals, an odd/even oscillation in the values of the diffusion barriers exists, with the monomers and trimers being more mobile than the dimers and the tetramers. This is due to the doublet spin state and the consequent fluxional character of the odd nuclearities, which are thus able to rearrange their configuration without significant loss of metallic energy, simultaneously optimizing the interaction with the surface. In passing, we note that it can be hypothesized that bigger clusters are also mobile enough on the surface to contribute to the growth process through diffusion processes (work in progress).

3.5. LDA results for gold

In the case of gold, it is known that a change of the xc-functional can sometimes translate into a qualitative change in the theoretical predictions [59]–[61]. To increase our confidence about the soundness of our results, we have thus repeated (only for the Au clusters) the static and dynamics analysis discussed above by using the LDA xc-functional instead of the PBE xc-functional. The LDA xc-functional, in fact, it is thought to better describe the gold metallic bond [59]–[61]. The analysis of the configurations from monomer to tetramer is reported in table 3, while the values of the diffusion barriers are reported in table 4.

A general trend which can be immediately evinced from the results in tables 3 and 4 is that the adhesion energies are increased, in particular the component due to the chemical interaction between the metal atoms and the surface. For the dimer, for example, we see that the energy difference between the ground-state upright configuration and the horizontal configuration is reduced from 0.87 eV (PBE) to 0.74 eV (LDA): although the metallic bond is strengthened by the use of LDA, in the horizontal configuration the inter-metal distance is elongated with respect

Table 4. The values of the energy barriers for the various diffusion mechanisms considered in the text are reported for Au_N ($N = 1$–4) clusters, as calculated using the LDA xc-functional.

Cluster	Mechanism	Barrier (eV)
Au_1	Monomer hopping	0.28
Au_2	Dimer hopping	0.75
Au_2	Dimer leapfrog	> 0.74
Au_3	Trimer walking	0.30
Au_4	Tetramer walking	0.72
Au_4	Tetramer rocking/rolling along [100]	0.73
Au_4	Tetramer rocking/rolling along [110]	0.66

to the equilibrium value (by about 0.1 Å), in order to exploit the direct interaction with the two oxygen ions of the terrace. On the other hand, in the upright configuration, the polarization contribution due to the metal-on-top effect is not increased as much as the direct interaction, and the energy difference is thus decreased. At the same time, the vertical configuration atop the hollow site, in which the chemical bond is reduced, is destabilized (from 0.62 to 0.75 eV) and is almost isoenergetic with the horizontal configuration. Another indication that the direct interaction is strongly increased by the use of LDA is given by the larger values of the distortion energies: in the ground-state of the tetramer, for example, we have a distortion energy of 1 eV and, at the same time, a remarkable increase in the adhesion energy value. In general, we can conclude that, at the LDA level, in the interplay between metallic bond and metal–surface interaction, the latter prevails, with the additional qualification of an increased importance of the direct 'chemical' interaction with the surface with respect to the polarization (metal-on-top) effect. This also translates into a general increase of the diffusion energy barriers, mainly due to the increased importance of the chemical interaction with the surface, which destabilizes the hollow sites with respect to the epitaxial oxygen sites, and thus typically the saddle point configurations with respect to the ground-states configurations. This increase brings, for example, the energy barrier for the monomer hopping to 0.28 eV, a value which is anyway within the experimentally determined range: 0.2–0.3 eV [62]. It thus seems that—contrary to the Cu/MgO(100) case [41]—the DF approach does not overestimate the metal–surface interaction, and thus the diffusion energy barrier, for Au/MgO(100). Further study is needed to clarify this point.

Apart from these considerations, however, the use of LDA does not introduce a qualitative change in the picture drawn in the previous discussion. The values of the diffusion energy barrier are generally larger and we still observe an odd/even oscillation in these values as a function of the nuclearity of the metal cluster.

3.6. Comparison with experiment

In a previous study, the diffusion barriers for small clusters of palladium absorbed on a regular (100) MgO surface have been calculated using the same methodology as applied here [27]. From these results, monomers and trimers diffuse with the same mechanism as gold and silver, i.e., monomer hopping and trimer walking, with barriers of 0.39 and 0.30 eV, respectively (also in this case the high-spin state of the trimer and its consequent fluxionality decrease the diffusion

barrier with respect to monomer hopping). The dimer diffuses via a dimer rotation mechanism with a barrier of 0.39 eV. The tetramer is absorbed on the surface as a tetrahedron [58] and diffuses via a rolling mechanism (different from that described here) with a barrier of 0.38 eV.

The values found for the three metals suggest that the order of mobility on the regular surface is Pd $\approx$ 0.38 eV $<$ Au $\approx$ 0.22 eV $<$ Ag $\approx$ 0.10 eV, in a corresponding approximate ratio of 3–4 : 2 : 1, following the decreasing strength of the metal–surface interaction. This ordering is in qualitative agreement with 'effective energy barriers' derived from recent molecular beam epitaxy (MBE) experiments [21]. In these experiments, the density of the metal islands grown on the regular surface is measured as a function of temperature and interpolated using an Arrhenius law, i.e., an exponential decrease of the density as a function of temperature. The empirical effective energy barriers of the Arrhenius curve determined from these experiments are 0.22/0.16 eV for Pd, 0.12 eV for Au and 0.08 eV for Ag. Even though the interpretation of these energy barriers is not immediate, as several mechanisms can contribute to metal island growth (diffusion, detrapping from defects and Ostwald ripening, etc), the reasonable agreement between these values and the diffusion energy barriers calculated in the present study leads us to conclude that the experimentally determined values are intimately related to diffusion processes on the surface.

4. Conclusions

The lowest energy structures and the diffusion barriers of small M_N (N = 1–4) Ag and Au clusters absorbed on the regular MgO (100) surface are investigated via DF calculations, using the PBE xc-functional for both Ag and Au clusters and the LDA xc-functional for Au clusters only.

Concerning the lowest-energy structures, in agreement with previous studies [26, 36, 37], we find a predominance of planar configurations with the plane of the cluster perpendicular to the surface. This is rationalized in terms of a strong metal-on-top effect, particularly important for coinage metal clusters, due to the weakness of the direct metal–surface interaction and the large polarizability of the valence s electrons. The structures of the absorbed clusters thus resemble those in the gas-phase (which are also planar in this size range), even though the deformation with respect to the non-symmetric gas-phase structures can sometimes be appreciable in the case of gold.

Concerning the diffusion mechanisms, we find a variety of possibilities, some of which have been already previously described, such as monomer hopping (Ag and Au), dimer leapfrog (Ag_2, see Cu_2 in [26]) and trimer walking (Au_3 and Ag_3, see Pd_3 in [27, 28]); whereas some are novel, such as dimer hopping (Au_2), and tetramer walking (Ag_4) or tetramer rocking/rolling (Au_4). Diffusion being a subtler process than absorption, one finds appreciable differences between silver and gold. An analysis of the corresponding energy barriers also shows that trimers can diffuse at least as fast as monomers, while tetramers and, especially in the case of gold, dimers present somewhat higher barriers. Even though not dramatic, this even–odd alternation might be a general feature of Ag–Au/oxide systems and is anyway sufficiently large to be in principle exploitable in MBE soft-landing experiments at sufficiently low temperature [63, 64]. The main conclusion of the present study is, anyway, that at the temperatures of the MBE experiments [21] small clusters definitely contribute to the metal mobility on the MgO (100) surface, and that the calculated diffusion energy barriers compare reasonably well with the values extracted from the analysis of the MBE experimental data,

so that the effective energy barriers derived from this analysis should be essentially correlated with diffusion processes.

Finally, we note that the use of the LDA xc-functional for Au does not qualitatively modify the results, except for a general increase in the adhesion energies and diffusion energy barriers.

Acknowledgments

We acknowledge financial support from the Italian CNR for the project '(Supra-) Self-Assemblies of Transition Metal Nanoclusters' within the framework of the ESF EUROCORES SONS, and from the European Community Sixth Framework Project for the STREP Project 'Growth and Supra-Organization of Transition and Noble Metal Nanoclusters' (contract no. NMP-CT-2004-001594).

References

[1] Henry C R 1998 *Surf. Sci. Rep.* **31** 235
[2] Freund H J 2002 *Surf. Sci.* **500** 271
[3] Hutchings G J and Haruta M 2005 *Appl. Catal.* A **291** 2
[4] Campbell C T 1997 *Surf. Sci. Rep.* **27** 1
[5] Remediakis N, Lopez N and Norskov J K 2005 *Appl. Catal.* A **291** 13
[6] Chen M S and Goodman D W 2004 *Science* **306** 252
[7] Häkkinen H, Abbet S, Sanchez A, Heiz U and Landman U 2003 *Angew. Chem. Int. Edn. Engl.* **42** 1297
[8] de Oliveira A L, Wolf A and Schüth 2001 *Catal. Lett.* **73** 157
[9] Wang R, Hao J, Guo X, Wang X and Liu X 2004 *Stud. Surf. Sci. Catal.* **154** 2632
[10] Lim D C, Lopez-Salido I and Kim Y D 2005 *Surf. Sci.* **598** 96
[11] Nepijiko S A, Ievlev D N and Schulze W 2003 *Eur. Phys. J.* D **24** 115
[12] Celep G *et al* 2004 *Phys. Rev.* B **70** 165409
[13] Zheng J and Dickson R M 2002 *J. Am. Chem. Soc.* **124** 13982
[14] Brongersma M L 2003 *Nat. Mater.* **2** 296
[15] Moseler M, Häkkinen H and Landman U 2003 *Phys. Rev. Lett.* **89** 176103
[16] Yudanov I, Pacchioni G, Neyman K and Rösch N 1997 *J. Phys. Chem.* B **101** 2786
[17] Matveev A V, Neyman K, Yudanov I and Rösch N 1999 *Surf. Sci.* **426** 123
[18] Campbell C T and Starr D E 2002 *J. Am. Chem. Soc.* **124** 9215
[19] Henry C R 1996 *Mater. Sci. Eng. A: Struct.* **217/218** 239
[20] Haas G, Menck A, Brune H, Barth J V, Venables J A and Kern K 2000 *Phys. Rev.* B **61** 11105
[21] Højrup-Hansen K, Ferrero S and Henry C R 2004 *Surf. Sci.* **226** 167
[22] Revenant C, Renaud G, Lazzari R and Jupille J 2006 *Nucl. Instrum. Methods* B **246** 112
[23] Kyuno K, Golzhauser A and Ehrlich G 1998 *Surf. Sci.* **397** 191
[24] Linderoth T R, Horch S, Petersen L, Helveg S, Lægsgaard E, Stensgaard I and Besenbacher F 1999 *Phys. Rev. Lett.* **82** 1494
[25] Montalenti F and Ferrando R 1999 *Phys. Rev. Lett.* **82** 1498
[26] Musolino V, Selloni A and Car R 1999 *Phys. Rev. Lett.* **83** 3242
[27] Barcaro G, Fortunelli A, Nita F and Ferrando R 2005 *Phys. Rev. Lett.* **95** 246103
[28] Xu L, Henkelman G, Campbell C T and Jónsson H 2005 *Phys. Rev. Lett.* **95** 146103
[29] Xu L, Henkelman G, Campbell C T and Jónsson H 2006 *Surf. Sci.* **600** 1351
[30] Abbet S, Sanchez A, Heiz U, Schneider W D, Ferrari A M, Pacchioni G and Rösch N 2000 *J. Am. Chem. Soc.* **122** 3453

[31] Sanchez A, Abbet S, Heiz U, Schneider W D, Häkkinen H, Barnett R N and Landman U 1999 *J. Phys. Chem.* A **103** 9573
[32] Molina L M and Hammer B 2004 *Phys. Rev.* B **69** 155424
[33] Walter M and Häkkinen H 2005 *Phys. Rev.* B **72** 205440
[34] Neyman K M, Inntam C, Nasluzov V A, Kosarev R and Rösch N 2004 *Appl. Phys.* A **78** 823
[35] Inntam C, Moskaleva L, Neyman K M, Nasluzov V A and Rösch N 2006 *Appl. Phys.* A **82** 181
[36] Inntam C, Moskaleva L, Yudanov I V, Neyman K M, Nasluzov V A and Rösch N 2006 *Chem. Phys. Lett.* **417** 515
[37] Barcaro G and Fortunelli A 2005 *J. Chem. Theory Comput.* **1** 972
[38] Del Vitto A, Pacchioni G, Delbecq F and Sautet P 2005 *J. Phys. Chem.* B **109** 8040
[39] Zhukovskii Y F, Kotomin E A, Fucks D and Dorfman S 2004 *Superlatt. Microstruct.* **36** 63
[40] Yang Z, Wu R, Zhang Q and Goodman D W 2002 *Phys. Rev.* B **65** 155407
[41] Lopez N, Illas F, Rösch N and Pacchioni G 1999 *J. Chem. Phys.* **110** 4873
[42] Bogicevic A and Jennison D R 2002 *Surf. Sci.* **515** L481
[43] Ouahab A, Mottet C and Goniakowski J 2005 *Phys. Rev.* B **72** 035421
[44] Coquet R, Hutchings G J, Taylor S H and Willock D J 2006 *J. Mater. Chem.* **16** 1978
[45] Baroni S, Del Corso A, de Gironcoli S and Giannozzi P Online at http://www.pwscf.org
[46] Perdew J P, Burke K and Ernzerhof M 1996 *Phys. Rev. Lett.* **77** 3865
[47] Jones R O and Gunnarsson O 1989 *Rev. Mod. Phys.* **61** 689
[48] Mills G and Jónsson H 1994 *Phys. Rev. Lett.* **72** 1124
[49] Henkelman G, Uberuaga B P and Jónsson H 2000 *J. Chem. Phys.* **113** 9901
[50] Eyring H 1935 *J. Chem. Phys.* **3** 107
[51] Mottet C, Barcaro G and Fortunelli A, unpublished
[52] Becke A D 1993 *J. Chem. Phys.* **98** 5648
[53] Barcaro G and Fortunelli A 2006 *J. Phys. Chem.* B **110** 21021
[54] Yulikov M, Sterrer M, Heyde M, Rust H-P, Risse T, Freund H-J, Pacchioni G and Scagnelli A 2006 *Phys. Rev. Lett.* **96** 146804
[55] Pyykkö P 2004 *Angew. Chem. Int. Edn. Engl.* **43** 4412
[56] Vervisch W, Mottet C and Goniakowski J 2002 *Phys. Rev.* B **65** 245411
[57] Ferrari A M, Xiao C, Neyman K M, Pacchioni G and Rösch N 1999 *Phys. Chem. Chem. Phys.* **1** 4655
[58] Giordano L and Pacchioni G 2005 *Surf. Sci.* **575** 197
[59] Aprá E, Ferrando R and Fortunelli A 2006 *Phys. Rev.* B **73** 205414
[60] Fernandez E M, Soler J M, Garzón I L and Balbas L C 2004 *Phys. Rev.* B **70** 165403
[61] Bonačič-Koutecky V, Burda J, Mitrič R, Ge M, Zampella G and Fantucci P 2002 *J. Chem. Phys.* **117** 3120
[62] Yulikov M, Sterrer M, Risse T and Freund H J, submitted
[63] Moseler M, Häkkinen H and Landman U 2002 *Phys. Rev. Lett.* **89** 176103
[64] Antonietti J-M, Michalski M, Heiz U, Jones H, Lim K H, Rösch N, Del Vitto A and Pacchioni G 2005 *Phys. Rev. Lett.* **94** 213402